

Nanoindentation creep and glass transition temperatures in polymers

Ben D Beake,¹ Gerard A Bell,^{1,2} Witold Brostow^{3*} and Wunpen Chonkaew³

¹Micro Materials Ltd, Unit 3 Wrexham Technology Park, Wrexham LL13 7YP, UK

²Department of Metallurgy and Materials, University of Birmingham, Edgbaston, Birmingham B15 2TT, UK

³Laboratory of Advanced Polymers & Optimized Materials (LAPOM), Department of Materials Science and Engineering, University of North Texas, Denton, TX 76203-5310, USA

Abstract: The nanoindentation creep behaviour of several different polymers has been investigated. The extent of creep ε is represented by the Chudoba and Richter equation: $\varepsilon = \varepsilon_e \ln(\varepsilon_r t + 1)$, where t is the loading time and ε_e and ε_r are material constants. Creep was determined in this way for a variety of polymers at $T_{\text{exper}} = 301.7 \text{ K}$. Some of the materials studied were far above, some far below and some near their glass transition temperatures T_g . The creep rate ε_r was plotted as a function of $y = (T_g - T_{\text{exper}})$; a single curve was obtained in spite of a large variety of chemical structures of the polymers. The $\varepsilon_r = \varepsilon_r(y)$ diagram can be divided into three regions according to the chain mobility. At large negative y values, the creep rate is high due to the liquid-like behaviour. At large positive y values in the glassy region, the creep rate is higher than that in the negative y -value region; the creep mechanism is assigned to material brittleness and crack propagation. In the middle y range there is a minimum of ε_r . These results can be related to glassy and liquid structures represented by Voronoi polyhedra and Delaunay simplices. The latter form clusters; in the glassy material there is a percolative Delaunay cluster of nearly tetrahedral high-density configurations. The creep mechanism here is related to crack propagation in brittle solids. In the liquid state there is a different percolative Delaunay cluster formed by low-density configurations, which, as expected, favour high creep rates.

© 2007 Society of Chemical Industry

Keywords: creep; glass transition; nanoindentation; Voronoi polyhedra; Delaunay simplices

INTRODUCTION

When materials are subjected to a constant load for a period of time, a time-dependent deformation – namely creep – is observed. Creep is an important phenomenon not only for describing viscoelasticity of polymer-based materials (PBMs) but also in the design of products made from PBMs. Thus, creep affects significantly service performance and service life of PBMs.^{1–8} A better understanding of creep would clearly improve our ability to enhance the service performance of polymers, polymer-containing composites and hybrids.

We have performed creep testing of several polymeric materials using nanoindentation. The technique has been used to characterize mechanical properties such as hardness and elastic modulus of a wide variety of materials, although there is still some debate about whether it is possible to determine meaningfully the hardness of strongly time-dependent materials.^{9–13} Results obtained from nanoindentation have an important advantage over those from conventional methods: they can separate creep from wear. The nanoindentation has been performed with a Micro Materials NanoTest system which allows for

very high strain rate indentation in addition to more conventional quasi-static indentation, thus enabling comparison between PBM properties at high and low strain rates. Results to date have shown that it is not always possible to infer properties at high strain rates from measurements obtained at lower strain rates.^{13–15}

In previous work^{6,15–18} we concentrated on the exact fitting of the initial phase (0–60 s) of indentation creep results to a simple equation proposed by Chudoba and Richter:¹⁹

$$\varepsilon = \varepsilon_e \ln(\varepsilon_r t + 1) \quad (1)$$

where ε is the increase in depth at maximum load, t is the loading time and ε_e and ε_r are material constants determining the extent of creep and the rate of creep, respectively. Since the quality of the fit of experimental results to Eqn (1) is very good, the method has been used to identify subtle changes in creep behaviour with additive loading or density of cross-linking of a range of polymer systems such as acrylonitrile/butadiene/styrene (ABS),¹⁵ poly(ethylene terephthalate) (PET),^{15,17} poly(ethylene oxide) (PEO) + clay^{6,15} and cross-linked plasma polymerized hexane films.^{16,18} The initial depth prior to

* Correspondence to: Witold Brostow, Laboratory of Advanced Polymers & Optimized Materials (LAPOM), Department of Materials Science and Engineering, University of North Texas, Denton, TX 76203-5310, USA

E-mail: brostow@unt.edu

Contract/grant sponsor: Robert A Welch Foundation; contract/grant number: B-1203

Contract/grant sponsor: Royal Thai Fellowship

(Received 22 May 2006; revised version received 26 September 2006; accepted 24 October 2006)

Published online 13 March 2007; DOI: 10.1002/pi.2207

the hold segment (see below) was kept constant by means of a depth-terminated nanoindentation load ramp.

We know from the viscoelasticity theory that creep, including its time dependence, is controlled in polymeric materials by the free volume available for molecular (segmental) motions.^{1–8} According to one explanation, around the glass transition temperature T_g heating creates sufficient free volume v^f to allow molecules to move relative to one another.²⁰ As advocated by Flory²¹ and others, the free volume can be calculated as

$$v^f = v - v^* \quad (2)$$

where v is the specific volume (usually in $\text{cm}^3 \text{g}^{-1}$) and v^* is the incompressible or hard core volume obtainable from $v(T, P)$ results via an equation of state such as that developed by Hartmann and Haque.²² We postulated that a correlation between the parameters in Eqn (1) and T_g (a point representing the glass transition region) would exist. We keep in mind that the location of T_g is determined by v^f changes.

EXPERIMENTAL

Materials

Materials selected were based on wide ranges of their chemical structures, mechanical properties and a variety of applications. Polystyrene (PS) was purchased from Aldrich Chemicals Company. Santoprene[®] was supplied by Advanced Elastomer Systems, Houston, TX. Santoprene is a thermoplastic elastomer, containing ethylene propylene diene monomer (EPDM) and polypropylene (PP) copolymer. Surlyn[®] 8140 was supplied by EI du Pont de Nemours, Wilmington, DE; it is a thermoplastic resin, an advanced ethylene/methacrylic acid (E/MAA) copolymer, in which the MAA groups have been partially neutralized with sodium ions. Polycarbonate (PC), acrylonitrile-butadiene-styrene (ABS) copolymer and polytetrafluoroethylene (PTFE) were supplied by Dow Chemical Company. PP was supplied by Phillips. Low-density polyethylene (LDPE) was supplied by Huntsman. Polyethersulphone (PES) was supplied by Solvay Engineered Plastics.

Nanoindentation creep testing

A NanoTest System manufactured by Micro Materials was used for the nanoindentation creep testing; the technique has been described previously.^{6,13–18} Briefly, the machine is a pendulum-based depth-sensing system, with the sample mounted vertically and the load applied electromagnetically as shown schematically in Fig. 1. Current in the coil causes the pendulum to rotate on its frictionless pivot so that the diamond probe penetrates the film surface. We used a Berkovich-type three-sided pyramidal indenter, angle 65.3° , with an equivalent conical indenter

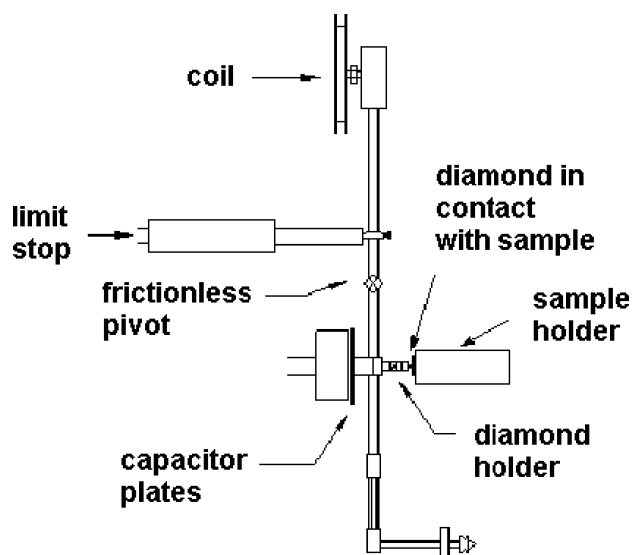


Figure 1. Schematic of the NanoTest system.

angle of 70.3° . The equivalent angle gives the same area-to-depth ratio as the actual Berkovich indenter.

Test probe displacement was measured with a parallel plate capacitor achieving sub-nanometre resolution. Indentations were load-controlled to 5 mN maximum load at 0.2 mN s^{-1} , followed by a 60 s holding period at this peak load for creep testing. Twenty tests were performed on each of the nine polymer samples at various locations on the surface of a given sample.

Analysis methodology

As already mentioned, Eqn (1) has been used previously^{6,15–18} to fit the creep behaviour and has been found to indicate sometimes rather subtle differences in the rate and extent of the time-dependent deformation; ε_e is interpreted as an extent term and ε_r as a rate term. Normalizing, that is dividing ε_e by the initial deformation at the first indentation $\varepsilon(0)$, provides a dimensionless parameter, $\varepsilon_e/\varepsilon(0)$, which enables comparison of different materials. In our earlier work, the initial deformation was set equal by means of a depth-terminated load ramp, although values of $\varepsilon_e/\varepsilon(0)$ themselves were not explicitly quoted. Somewhat similarly, Berthoud *et al.*²³ analysed the logarithmic behaviour using an Eyring-type creep law in terms of scalar stress and strain for a spherical indenter. According to them, the fractional increase in depth (i.e. strain) $\varepsilon/\varepsilon(0)$ is

$$\varepsilon/\varepsilon(0) = m_{\text{eff}} \ln(t/\tau + 1) \quad (3)$$

where $\tau = 1/\varepsilon_r =$ creep time and $m_{\text{eff}} = \varepsilon_e/\varepsilon(0) =$ strain rate sensitivity. We have chosen to fit the first 60 s of the experimental creep data to a modification of Eqn (1) such that quantities on both sides are dimensionless:

$$\varepsilon/\varepsilon(0) = [\varepsilon_e/\varepsilon(0)] \times \ln(\varepsilon_r t + 1) \quad (4)$$

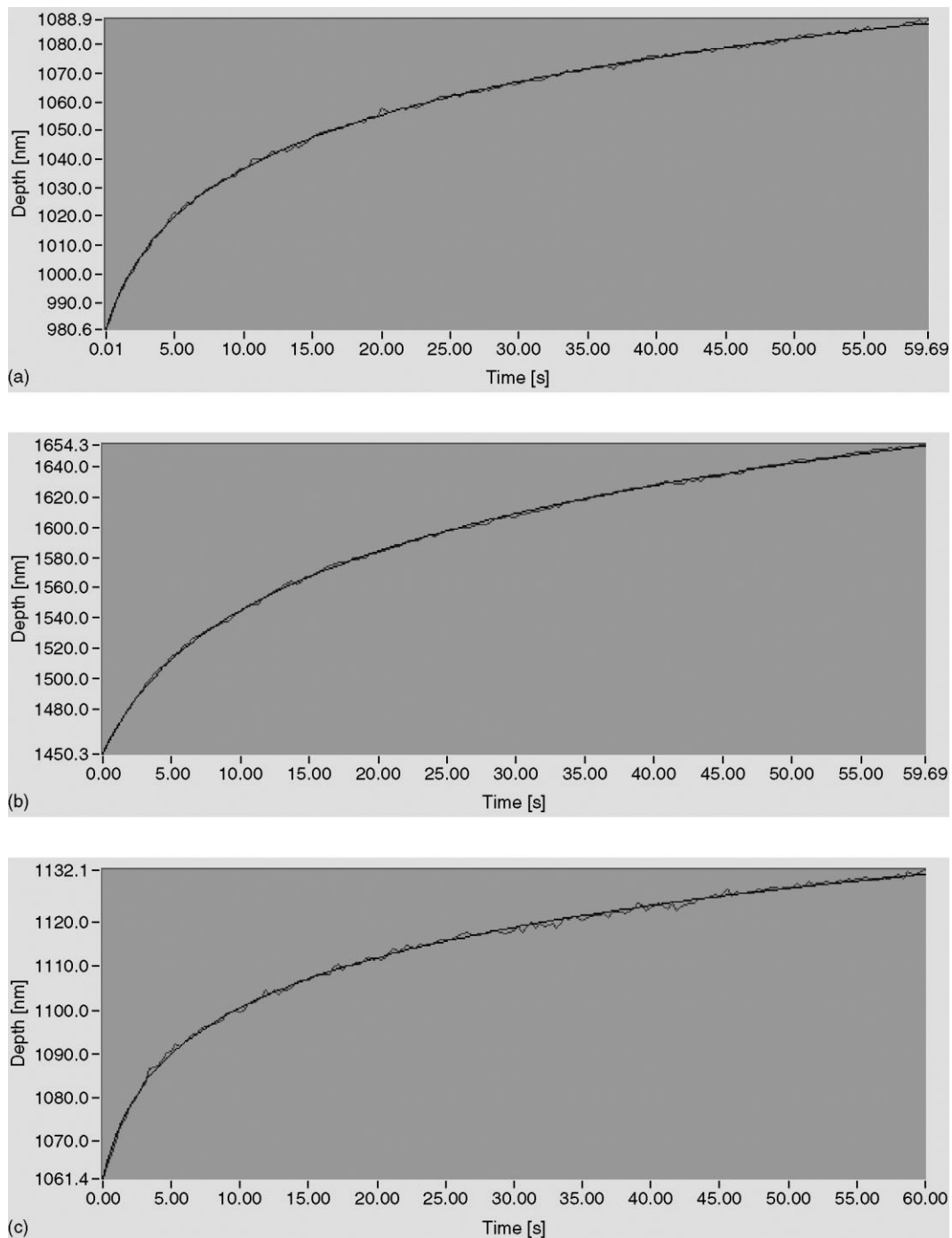


Figure 2. Illustrative creep results for (a) PS, (b) PP and (c) PES.

It has been shown previously²⁴ that ε_r varies with the loading time while $\varepsilon_r/\varepsilon(0)$ is relatively insensitive to the loading time.

RESULTS

Although indentation testing is possible at non-ambient temperatures (25–750 °C) with the Nano-Test, in this study all the indentation creep properties were determined at a temperature close to room temperature, $T_{\text{exper}} = 307.1$ K. Illustrative creep test results for PS, PP and PES are shown in Fig. 2. In all cases the fit to Eqn (4) is excellent. The results

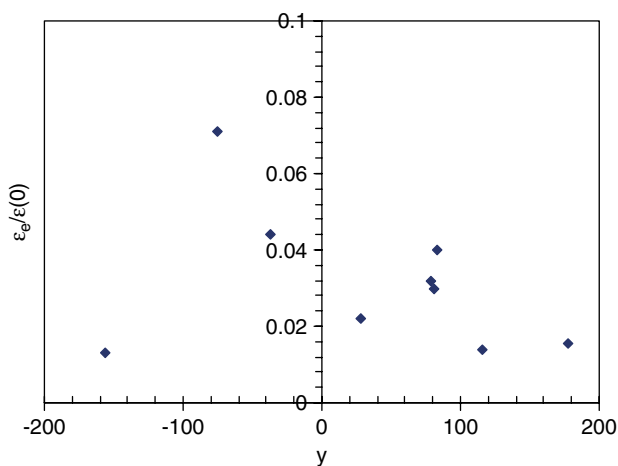
are summarized in Table 1. By testing close to room temperature, on purpose some polymers studied are far above, some far below and some near the glass transition temperature. Since large differences in behaviour are expected far below and far above T_g , we define

$$y = T_g - T_{\text{exper}} \quad (5)$$

to represent numerically the distance from the glass transition temperature. Clearly negative y values correspond to rubber- or liquid-like behaviour and positive y values to glassy behaviour.

Table 1. The creep parameters for each polymer and the glass transition temperatures

Polymer	$\varepsilon_e/\varepsilon(0)$	ε_r	T_g ($^{\circ}\text{C}$)
PES	0.0155	0.939	206.4
PC	0.0139	1.028	144.8
ABS	0.0296	0.521	109.4
PS	0.0320	0.477	107.5
Surlyn	0.0220	0.395	57.4
PTFE	0.0400	0.442	111.6
PP	0.0440	0.325	-7.8
LDPE	0.0130	0.696	-126.8
Santoprene	0.0710	0.155	-46

**Figure 3.** Strain rate sensitivity $\varepsilon_e/\varepsilon(0)$ as a function of y as defined by Eqn (5).

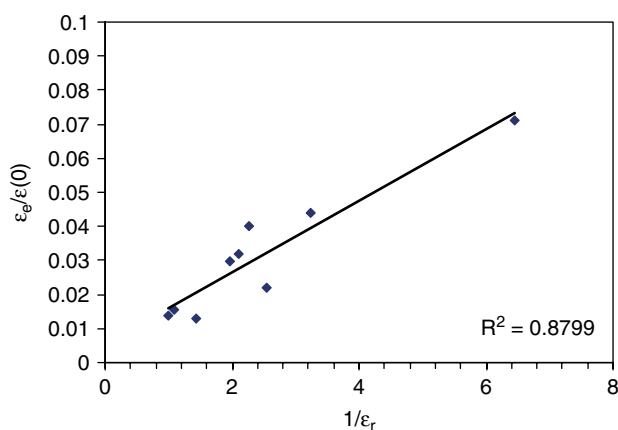
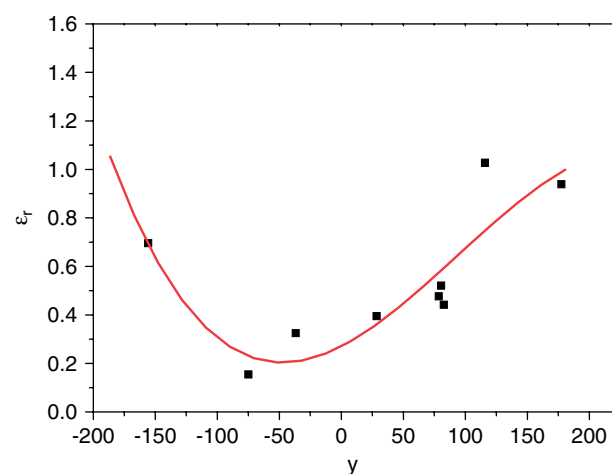
ANALYSIS OF THE RESULTS

Results of the first attempt to investigate the creep parameters are shown in Fig. 3. The plot of $\varepsilon_e/\varepsilon(0)$ as a function of y is fairly complex. A maximum seems to be present. Previously²⁴ a complex relationship has been observed also between $\varepsilon_e/\varepsilon(0)$ and $T - T_g$ for a range of amorphous and semi-crystalline samples. In particular, ultrahigh-molecular-weight PE (UHMWPE) showed large values of $\varepsilon_e/\varepsilon(0)$ despite being far from T_g , in sharp contrast to LDPE which exhibits low $\varepsilon_e/\varepsilon(0)$. Differences in crystallinity may be responsible for this.

In turn, we now consider the strain rate sensitivity as a function of the creep time. Figure 4 shows such a plot. In this case a clear correlation is found. An inspection of earlier data indicates that this correlation applies to a variety of polymer systems.

Finally, we return to our considerations based on the free volume defined by Eqn (2). Large negative values of y defined by Eq. (5) mean that we are far above T_g in the liquid or rubbery region. This implies high v^f values, consequently large chain mobility, and thus high creep rate ε_r . We plot $\varepsilon_r = \varepsilon_r(y)$ in Fig. 5.

Apart from some variations possibly caused by differences in crystallinity, a single $\varepsilon_r(y)$ curve has been obtained. Our initial assumption has been confirmed: the larger the negative values of y , the larger the creep rate.

**Figure 4.** Strain rate sensitivity $\varepsilon_e/\varepsilon(0)$ as a function of creep time $1/\varepsilon_r$. The perfect fit would correspond to $R^2 = 1$.**Figure 5.** Creep rate ε_r as a function of y defined by Eqn (5).

A more detailed analysis of Fig. 5 led us to divide the range of y into three different regions. One at large negative y values has already been explained. Another is at large positive y values, i.e. for T_g of polymers far above T_{exper} . Thus, polymers are glassy in this region. The mechanism, therefore, has to be vastly different. Large negative y values are caused by chain mobility but at large positive y values there is very little mobility. Thus, for $y > 50$ K or so, material brittleness and crack propagation are likely to be the dominant mechanisms of creep. We recall molecular dynamics simulations of crack propagation in two-phase polymers including polymer liquid crystals (PLCs).^{25,26}

In the middle of y range, that is for small y values, there is a minimum of ε_r . We do not have brittleness caused by large positive y values, nor high chain mobility due to high free volume for large negative y values. Thus, *both* creep-causing mechanisms are weak around $y = 0$. We recall also an earlier result for the PEO + clay system in which the value of ε_r decreases with increasing amount of clay, a consequence of a mobility decrease.⁶

Analysing the results presented in Fig. 5, we recall the application of the Voronoi–Delaunay approach²⁷ to understand the difference in the structure between

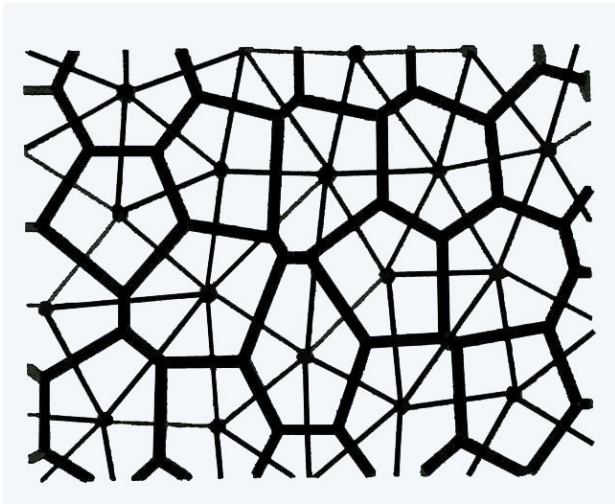


Figure 6. Voronoi–Delaunay tessellation for a set of points in two-dimensional space.

liquid and glassy phases.²⁸ This is based on a century-old approach of the Ukrainian mathematician Hrihory (Georges in his papers written in French published in a German journal) Voronoi.^{29,30} Consider a set of points in space. For simplicity let us limit ourselves to two dimensions. We draw lines connecting each point to its nearest neighbours; these are the thin lines in Fig. 6. The resulting structure is called the Delaunay simplex.

At the midpoint of each connecting line between any two points of the original structure a line is now drawn perpendicular to that connecting line (thick lines in Fig. 6). For every point we use the perpendicular lines to create the smallest polygon surrounding the point. The polygon is an intersection of half-spaces (for details see either the original papers^{29,30} or Brostow and Castaño²⁷) and is called the Voronoi polygon. It is a dual structure with respect to the Delaunay simplex.

In three dimensions we have the Voronoi polyhedra instead of polygons. For a given set of points, the complete set of the polyhedra is called the Voronoi diagram. There are computer methods of generating the Voronoi diagram for a given set of points.^{31,32} Dealing with amorphous (glassy) or liquid materials, we find that the Voronoi diagram characterizes the material structure. The points correspond to atoms (in metals, or for instance in argon), to ions, or in polymeric materials to single mers or to representative (statistical) mers.²¹ The Voronoi diagram approach is applicable to any materials including crystals. However, in crystals the results are equivalent to those given by classic crystallography. The connection between the Delaunay figures (constituents of the Delaunay simplex in Fig. 6) and the crystal cells is easy to see.

Methods of characterization of structures by the Voronoi polyhedra rely on the size distribution of the polyhedra, distribution of the numbers of faces, distributions (or averages) of the face surface areas, etc. A useful measure of the structure has been defined by

Medvedev and Naberukhin³³ and called tetrahedrity T_h . It can be calculated from the Delaunay simplex information as

$$T_h = \sum_{i>j} (l_i - l_j)^2 / 15 \langle l \rangle^2 \quad (6)$$

where l_i is the length of the i -th simplex edge and $\langle l \rangle$ is the average edge length value in the material. According to Eqn (6), for $T_h = 0$ we have a regular tetrahedron structure. Thus, the higher are the values of T_h , the larger are deviations from regular tetrahedrity.

It has been demonstrated³³ that liquids (our y negative) have monomodal histograms of relative frequency of occurrence versus T_h . There is a percolative cluster, with low local density and high mobility, going across the entire material. Thus, such a cluster tends to be deformed easily and favours high ε_r . This situation corresponds to the left branch of the curve in Fig. 5, with experimental points marked by asterisks.

In the glassy phase (y positive), the liquid-like cluster is absent.³³ There is a marked minimum in the histograms for $T_h \approx 0.016$. For $T_h < 0.016$ there is a different percolative cluster consisting of a nearly regular tetrahedral configuration with high segmental density. It seems plausible to assume that this T_h region corresponds in Fig. 5 to the central part of the diagram; it includes also some small negative y values. We are close to T_g on either side of $y = 0$; T_h is low, the tetrahedra nearly regular. For larger positive y values we see a jump to a higher ε_r plateau. As already argued above, the mechanism of creep here is similar in nature to crack propagation in brittle solids.

The present work is a part of a large programme aimed at understanding the tribology of PBMs using a variety of approaches.^{34–37} The conclusions of this study are also supported by results of nanoindentation creep tests at elevated temperatures.³⁸

ACKNOWLEDGEMENTS

Partial financial support was provided by the Robert A Welch Foundation, Houston (Grant B-1203) and also by the Royal Thai Fellowship, Bangkok (to WC) held at the University of North Texas.

REFERENCES

- 1 Ferry JD, *Viscoelastic Properties of Polymers*. Wiley, New York (1980).
- 2 Brostow W (ed.), *Failure of Plastics*. Hanser, Munich/New York (1986, 1989, 1992).
- 3 Nielson LE and Landel RF, *Mechanical Properties of Polymers and Composites*. Marcel Dekker, New York (1994).
- 4 Goldman AY, *Prediction of Deformation Properties of Polymeric and Composite Materials*. American Chemical Society, Washington, DC (1994).
- 5 Mazur S, in *Polymer Powder Technology*, ed. by Narkis M and Rosenzweig N. Wiley, Chichester/New York, chap. 8 (1995).
- 6 Beake BD, Chen S, Hull JB and Gao F, *J Nanosci Nanotech* 2:73 (2002).

- 7 Brostow W, *Mater Res Innovat* **3**:347 (2000).
- 8 Brostow W (ed.), *Performance of Plastics*. Hanser, Munich (2000).
- 9 Oliver W and Pharr G, *J Mater Res* **7**:1564 (1992).
- 10 Rau K, Singh R and Goldberg E, *Mater Res Innovat* **5**:151 (2002).
- 11 Tho KK, Swaddiwudhipong S, Lui SZ, Zeng K and Hua J, *J Mater Res* **19**:2498 (2004).
- 12 Alkorta J, Martinez-Esnaola JM and Gil-Sevillano J, *J Mater Res* **20**:432 (2005).
- 13 Beake BD, Zheng S and Alexander MR, *J Mater Sci* **37**:3821 (2002).
- 14 Beake BD and Leggett GJ, *Polymer* **42**:319 (2002).
- 15 Beake BD, Leggett GJ and Alexander MR, *J Mater Sci* **37**:4919 (2002).
- 16 Beake BD, Goodes SR, Smith JF and Gao F, *J Mater Res* **19**:237 (2004).
- 17 Juliano TF, VanLandingham MR, Tweedie CA and Van Vliet KJ, *Exp Mech*, DOI: 10.1007/s11340-006-8276-5.
- 18 Tweedie CA and Van Vliet KJ, *J Mater Res* **21**:1576 (2006).
- 19 Chudoba T and Richter F, *Surf Coat Technol* **148**:191 (2001).
- 20 Painter PC and Coleman MM, *Fundamentals of Polymer Science*. Technomic, Lancaster, PA (1994).
- 21 Flory PJ, *Selected Works*, vol. III. Stanford University Press, Stanford, CA (1995).
- 22 Hartmann B and Haque M, *J Appl Phys* **58**:2831 (1985).
- 23 Berthoud P, G'Sell C and Hiver JM, *J Phys D* **32**:2923 (1999).
- 24 Beake BD, *J Phys D* **39**:4478 (2006).
- 25 Brostow W, Cunha AM, Quintanilla J and Simões R, *Macromol Theory Simul* **11**:308 (2002).
- 26 Brostow W and Simões R, *J Mater Ed* **27**:19 (2005).
- 27 Brostow W and Castaño VM, *J Mater Ed* **21**:297 (1999).
- 28 Medvedev NN, Geiger A and Brostow W, *J Chem Phys* **93**:8337 (1990).
- 29 Voronoi G, *J Reine Angew Math* **134**:198 (1908).
- 30 Voronoi G, *J Reine Angew Math* **136**:67 (1909).
- 31 Brostow W, Dussault J-P and Fox BL, *J Comput Phys* **29**:81 (1978).
- 32 Brostow W, Chybicki M, Laskowski R and Rybicki J, *Phys Rev B* **57**:13441 (1998).
- 33 Medvedev NN and Naberukhin YI, *J Non-Cryst Solids* **94**:402 (1987).
- 34 Brostow W, Bujard B, Cassidy PE, Hagg HE and Montemartini PE, *Mater Res Innovat* **6**:7 (2002).
- 35 Brostow W, Damarla G, Howe J and Pietkiewicz D, *e - Polymers* **025**:1 (2004).
- 36 Bermudez MD, Brostow W, Carrion-Vilches J, Cervantes JJ, Damarla G and Perez JM, *e - Polymers* **003**:1 (2005).
- 37 Brostow W, Chonkaew W and Menard KP, *Mater Res Innovat* (in press).
- 38 Beake BD and Gray A, in preparation.